Strain Dependence of Critical Current in Internal Tin Process Nb_3Sn Strands

Sangjun Oh, Soo Hyeon Park, Chulhee Lee, Yongbok Chang, Keeman Kim, and Pyeong-Yeol Park

***Abstract*—The development of a high performance superconducting magnet requires a thorough understanding of the strain effect in the critical current density (J_c) of Nb_3Sn strands. A modified version of the WASP device is used for the investigation of the strain effect. The spring is made of BeCu alloy and is capable of applying strain up to 0.7% reversibly at 4.2 K. Several types of high performance Nb_3Sn strands ($J_c > 1000\ A/mm^2$ at 12 T and 4.2 K) have been developed using internal tin process. A comparative study on the axial strain dependence of the critical current is performed.**

***Index Terms*—Internal tin process Nb_3Sn strand, strain effect in the critical current density, WASP device.**

I. Introduction

Nb_3Sn SC strand is presently available mainly by two industrial fabrication processes, known as the 'bronze process' and the 'internal tin process'. Recently, internal tin process strands with J_c over 1000 A/mm^2 at 12 T and 4.2 K are available. Bronze process strands have also improved and are available with J_c over 750 A/mm^2. Because of their good mechanical stability, bronze process strands are preferred in applications operated in high strain environments. Since bronze process strands do not have enough Sn for A15 reaction, the un-reacted Nb, which enhances the mechanical stability of the filament, remains at the core part of the filament. It is also believed that internal tin process strands have larger Kirkendall voids [1], which degrade the superconducting performance under a highly stressed condition. However, the higher J_c characteristics of internal tin process strands are attractive in many large-scale applications and a thorough understanding of the strain effect is essential for the development of high strain resistant strands.

Due to the nature of the Nb_3Sn strand, a significant compressive strain is introduced in the Nb_3Sn superconducting strand during the cooling from the A15 reaction heat treatment temperature to the cryogenic temperature. Because of the difference in thermal expansion coefficients among constituent materials of the strand, there are tensile stresses on copper stabilizer and bronze material inside the diffusion barrier and compressive stresses on the Nb_3Sn and Nb filaments. For the case of a CICC (Cable-In-Conduit Conductor), the conduit, which is often made of stainless steel, also makes a significant contribution to the compressive strain in the Nb_3Sn filament. The strain in Nb_3Sn filaments affects superconducting properties such as critical current density (J_c), critical temperature (T_c), critical magnetic field (B_{c2}).

In order to investigate the strain effect, various kinds of internal tin process strands were manufactured by KAT(Kiswire Advanced Technology). In this paper, 4 types of strands are selected for comparisons. The basic specifications of the test samples, which have Sn alloy core with 1.5∼3 wt.% of Ti in their sub-elements, are summarized in Table I. Fig. 1 presents the cross-sectional views of KAT type A and B strands. The strand supplied by MELCO(Mitsubishi Electric Corporation) is used as a reference. A large amount of MELCO strand has been used for the construction of the KSTAR(Korea Superconducting Tokamak Advanced Research) superconducting magnet system.

TABLE I
Basic Specification of Strands

Strand name	Diameter	Cu/Non-Cu	number of filaments
MELCO	0.778 mm	1.5	224 x 37
KAT A	0.778 mm	1.0	219 x 19
KAT B	0.778 mm	1.0	219 x 37
KAT C	0.778 mm	1.0	223 x 37
KAT D	0.778 mm	1.0	165 x 19

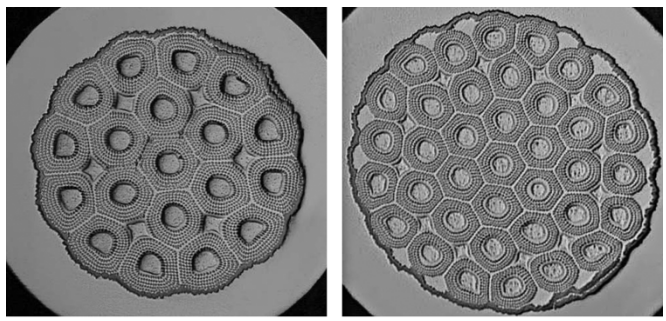

(a) (b)

Fig. 1. Cross-sectional views of KAT type A and B strands. (a) KAT type A strand; (b) KAT type B strand.

II. Experimental Procedure

Samples were heat treated on Ti-6Al-4V alloy mandrels. The temperature ramp rate during the heat treatment is 6°C/hour and there are three plateaus: 200°C for 5 hours to stabilize the temperature profile, 570°C, 200 hours to enhance the diffusion of Sn to Nb filament and 660°C, 240 hour for the A15 reaction of Nb_3Sn. To use MELCO strand for the verification of our strain effect measurement device as a reference, the heat treatment scenario for KSTAR CICC superconducting magnet was used except 460°C plateau between 200°C and 570°C ramping region. For the heat treatment of a CICC magnet, the plateau of

Manuscript received October 3, 2004. This work was supported by the Korean Ministry of Science and Technology.

S. Oh, S. H. Park, C. Lee, Y. Chang and K. Kim are with Korea Basic Science Institute, Daejeon, Korea 305-333 (e-mail: wangpi@kbsi.re.kr).

P.-Y. Park is with KAT (e-mail: pypark@kiswire.com).

Digital Object Identifier 10.1109/TASC.2005.849058

460°C for 100 hours is added to remove oxygen and contaminants from the cable inside the CICC. Although the plateau of 460°C may partially contribute to the enhancement of J_c, it is removed in this strand test for convenience.

After the heat treatment, samples for the strain effect measurement were carefully transferred from Ti-6Al-4V alloy mandrels to 2% beryllium doped copper alloy springs. Ti-6Al-4V alloy mandrels and 2% beryllium doped copper alloy springs have 0.5 mm deep 90 degree V-shape grooves on the surface. The V-shape groove in the beryllium copper alloy springs provides a larger contact area for strand soldering. As a result, a more uniform strain distribution along the strand is expected.

A modified version of the WASP(Walters Spring) probe using a beryllium copper alloy spring was made for the measurement of strain effects. The WASP device was first developed by C. R. Walter, *et al.* It can accommodate a longer sample and the sensitivity of critical current measurement is increased [2]. The strand sample is soldered to a spring, which usually made of material with high proportional limit of elasticity such as Ti-alloy or beryllium copper. When one end of the spring is rotated with respect to the other end, the strand sample on the spring is either stretched or compressed. The relation between the rotation angle and the strain can be calculated and is verified using attached strain gages [2], [3]. The direct investigation of microscopic strain in the strand by X-ray diffraction was also reported [4].

Our strain effect measurement probe is quite similar to that reported by N. Cheggour and D. P. Hampshire [3]. A 16 T Oxford magnet system with a large bore of 76 mm made it possible to use 6 mm diameter copper current leads. Up to 700 A critical current measurements at 4.2 K were possible.

A 4.5 turn spring was used and the strain-angle relation was measured at 4.2 K. The strain to angle ratio is 0.0124%/deg and it is reversible up to 0.73% for both compressive and tensile stresses. Total strand length on the spring spiral is 30 cm and the distance between voltage taps is 15 cm. Critical current is defined at the onset of 0.1 $\mu V/cm$. The sample current was applied by two parallel 350 A Chroma current sources and measured by a Danfysik current transducer. The voltage was measured with a Keithley 2182 nanovoltmeter.

III. Results and Discussion

Fig. 2 shows a typical I-V curve of the KAT strands at 12 T. The critical current at 0.1 $\mu V/cm$ criterion for KAT Type A(solid line) and KAT Type B(dotted line) are 1045 A/mm^2 and 977 A/mm^2, respectively. Inset shows the n-value of 25.4 for the KAT Type A, which was derived by fitting the I-V curve in the range between 0.1 and 1 $\mu V/cm$.

Magnetic field dependencies of J_c measured on the ITER barrels are plotted in Fig. 3. KAT type A, B, C samples show large critical current densities satisfying the increased Jc specification for ITER TF coil. The difference of thermal contraction between Ti alloy and beryllium copper alloy during the cooling down from room temperature to 4.2 K is ~0.125% [5]. Representative data for MELCO strand on beryllium copper alloy spring with 0.124% tensile strain in Fig. 3 are in good agreement with measured data using the ITER barrel.

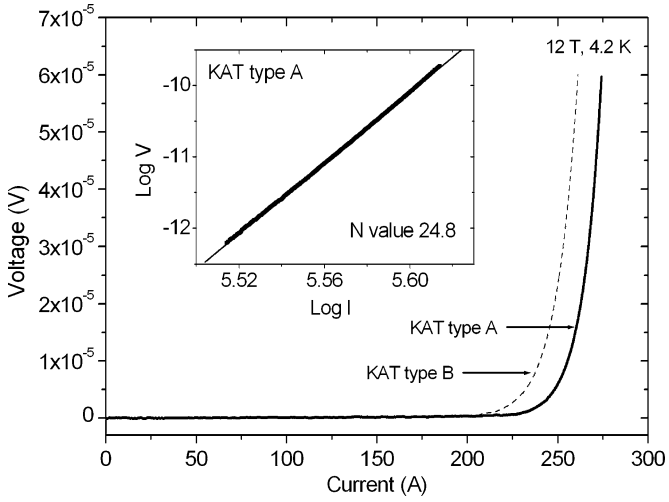

Fig. 2. Typical I-V curve for Jc measurement. Here KAT type A and B samples are measured at 12 T and 4.2 K. The inset shows a log-log plot of I-V in the range between 0.1 and 1 $\mu V/cm$.

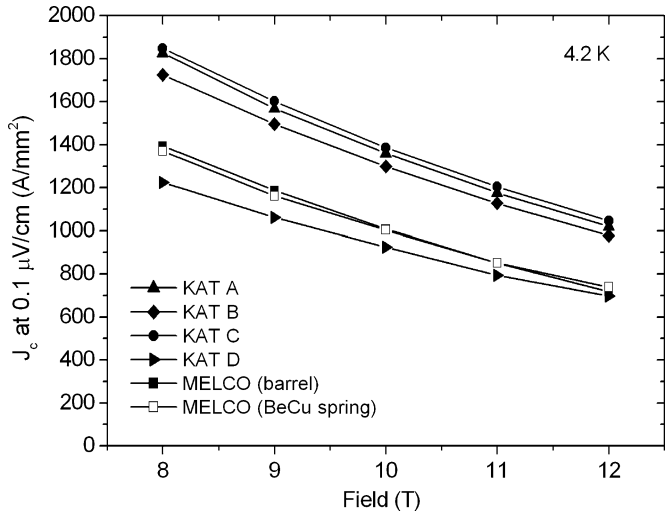

Fig. 3. J_c as a function of magnetic field. Solid data was measured with the ITER barrel and representative clear rectangular points were measure using a beryllium copper alloy spring under the 0.124% tensile strain.

Fig. 4 shows typical measurement data for the strain dependence of J_c. The marked points are the measured values for KAT Type A and B samples. After a few strain cycles from 0.73% to −0.73%, both strands show good repeatability. Kramer plots [6] for KAT Type A samples are shown in Fig. 5 and extrapolated upper critical fields are shown in Fig. 6. The maximum effective upper critical fields (B^*_{c2m}) at 4.2 K are summarized in Table II. B^*_{c2m} for all of internal tin process KAT strands investigated were larger than 31 T. The reason B^*_{c2m} are so high is because a Kramer extrapolation was used. These are not the actual upper critical field [7]–[9].

Fig. 7 shows the strain dependent Jc measurement data for KAT Type A sample at various applied fields. Solid lines are calculated using the Ekin's scaling law [10],

$$F_p(B,\varepsilon) = CB_{c2}(\varepsilon)^n f\left(\frac{B}{B_{c2}(\varepsilon)}\right),$$

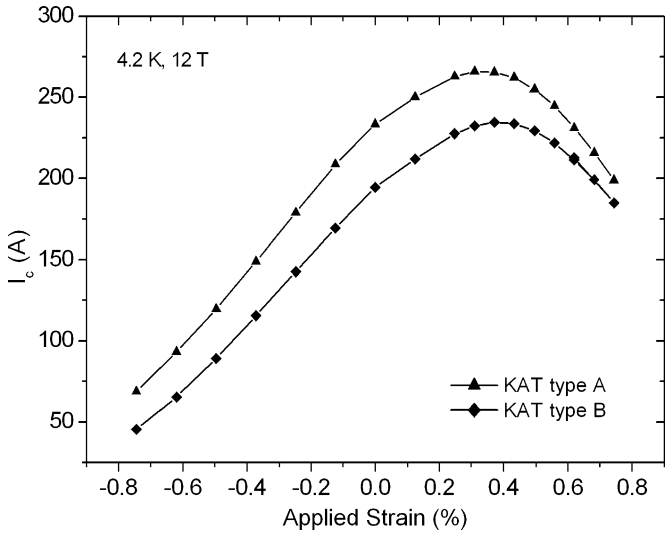

Fig. 4. Critical current as a function of applied strain for KAT type A and B strands at 12 T and 4.2 K. After a few cyclic loads of strain, data were reversible.

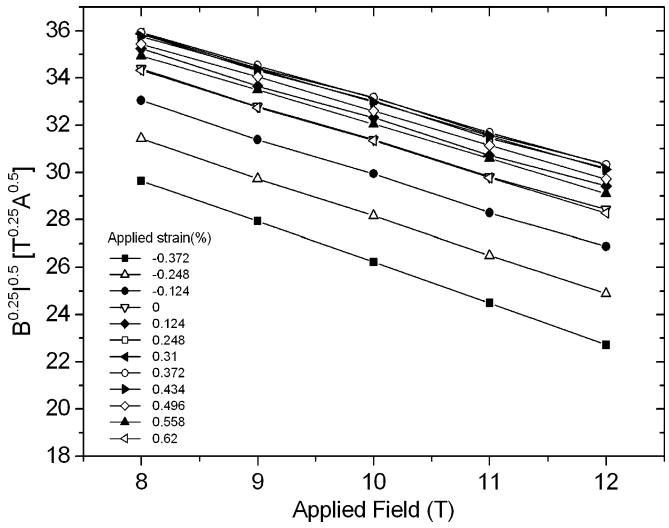

Fig. 5. Kramer plots for KAT type A samples.

where,

$$f\left(\frac{B}{B_{c2}(\varepsilon)}\right) = f(b) = b^p(1-b)^q,$$
$$B_{c2}(\varepsilon) = B_{c2m}\left(1 - a|\varepsilon_a - \varepsilon_m|^u\right).$$

The optimal constants for n, p, q and u were 1, 0.5, 2 and 1.7, respectively. The values of $p = 0.5$, $q = 2$ coincide with that given by Kramer's flux-line shearing model. However, for homogeneous ternary Nb_3Sn, a q parameter of 1.6 was reported when I_c is measured at fields above 16 T [7]. The strain-scaling constant a is listed in Table II. In the high compressive strain region, larger critical currents than expected from Ekin's scaling law are observed. For the KAT type B sample, a similar behavior was also observed. Since KAT Type A and B strands have relatively low Sn contents compare to Type C and D, their filaments are expected to have Nb cores after A15 reaction heat treatment [9]. The un-reacted Nb core might help the strand to have less strain sensitive characteristics at high compressive strain.

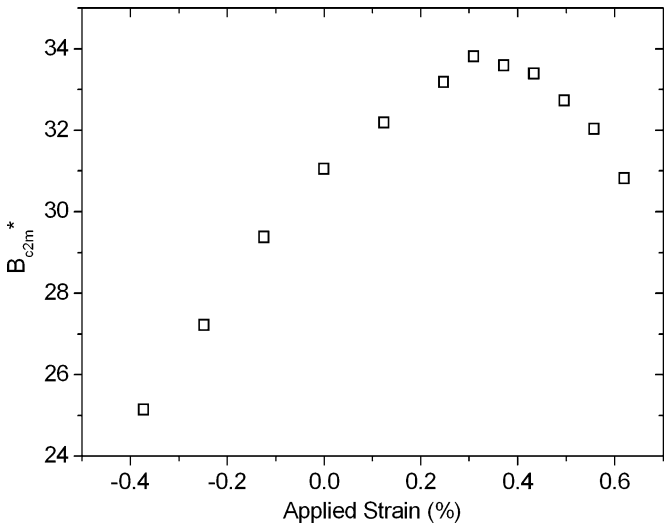

Fig. 6. Extrapolated upper critical field of KAT type A sample at various applied strain.

TABLE II
UPPER CRITICAL FIELDS AND EKIN'S SCALING PARAMETERS

Strand name	B_{c2m}*(4.2K)	a ($\varepsilon_a < \varepsilon_m$)	a ($\varepsilon_a > \varepsilon_m$)
MELCO	29.7	1250	2000
KAT A	33.8	1150	1700
KAT B	32.6	1400	1400
KAT C	31.1	1000	3500
KAT D	32.9	1000	1500

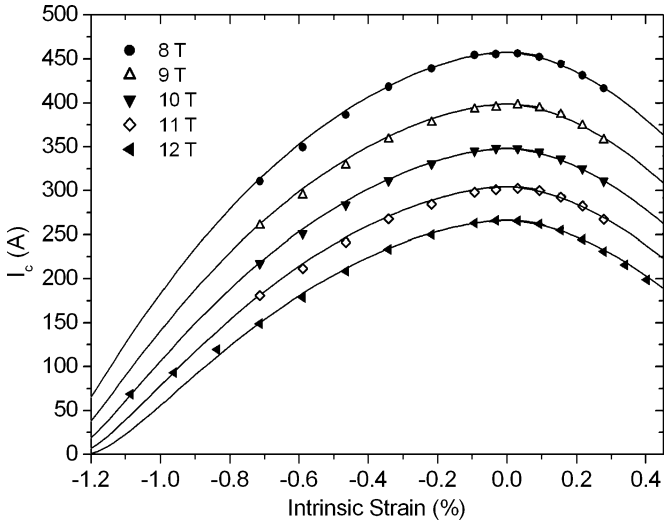

Fig. 7. Strain dependent Jc measurement data for KAT type A sample at various applied field. Lines are calculated with the Ekin's scaling law.

Though it requires further investigations, it is also expected to have high strain resistant characteristics in compressive transverse stress.

The comparison of strain dependence among various internal tin processed Nb_3Sn strands is illustrated in Fig. 8. The data are normalized for the maximum value of the each strand, where the intrinsic strain is defined to 0%. The reductions in J_c at -0.7% strain for KAT strands and MELCO strand are $\sim$45% and $\sim$53%, respectively.

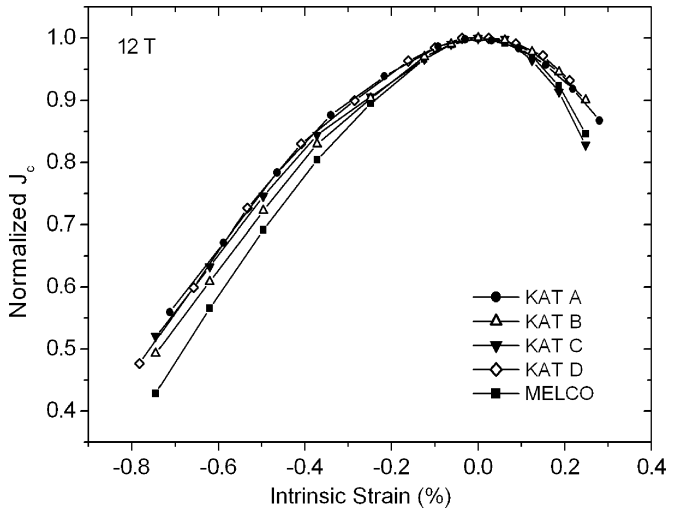

Fig. 8. Normalized Jc as a function of intrinsic strain for various strands at 12 T and 4.2 K.

IV. Conclusion

The axial strain dependency of the critical current has been studied for various internal tin processed Nb_3Sn strands using a modified version of WASP device. Though the effect of the transverse stress on the critical current still needs to be investigated, a well-designed internal tin processed Nb_3Sn SC strand shows a strong strain resistance enough for large-scale, high-field applications such as a superconducting tokamak fusion reactor.

References

[1] S. Nourbakhsh, Y. S. Hascicek, M. J. Goringe, and J. W. Martin, "On the presence of voids in bronze-route multi-filamentary Nb_3Sn superconducting wires," *J. Mater. Sci.*, vol. 17, p. 3204, 1982.

[2] C. R. Walters, I. M. Davidson, and G. E. Tuck, "Long sample high sensitivity critical current measurements under strain," *Cryogenics*, vol. 26, p. 406, 1986.

[3] N. Cheggour and D. Hampshire, "A probe for investigating the effects of temperature, strain, and magnetic field on transport critical currents in superconducting wires and tapes," *Rev. Sci. Instrum.*, vol. 71, p. 4521, 2000.

[4] B. ten Haken, A. Godeke, and H. H. J. ten Kate, "Investigation of microscopic strain by X-ray diffraction in Nb_3Sn tape conductors subjected to compressive and tensile strain," *Adv. Cryog. Eng. (Mat.)*, vol. 42, p. 1463, 1997.

[5] R. P. Reed and A. F. Clark, Eds., *Materials at Low Temperatures*. Metals Park, OH: American Society for Metals, 1983.

[6] E. J. Kramer, "Scaling laws for flux pinning in hard superconductors," *J. Appl. Phys.*, vol. 44, p. 1360, 1973.

[7] J. W. Ekin, "High-field flux pinning and the strain scaling law," in *Proc. Int'l. Symp. on Flux Pinning and Electromagnetic Properties in Superconductors*, T. Matsushita, K. Yamafuji, and F. Irie, Eds., Fukuoka, 1985, pp. 267–271.

[8] A. Godeke, M. C. Jewell, A. A. Golubov, B. Ten Haken, and D. C. Larbalestier, "Inconsistencies between extrapolated and actual critical fields in Nb_3Sn wires as demonstrated by direct measurements of H_{c2}, H^* and T_c," *Supercond. Sci. Technol.*, vol. 16, p. 1019, 2003.

[9] A. Godeke, M. C. Jewell, C. M. Fisher, A. A. Squitieri, P. J. Lee, and D. C. Larbalestier, The Upper Critical Field of Filamentary Nb_3Sn Conductors.

[10] J. W. Ekin, "Strain scaling law for flux pinning in practical superconductors. Part I: basic relationship and application to Nb_3Sn conductors," *Cryogenics*, vol. 20, p. 611, 1980.